Biological
Cybernetics

Study of neuronal gain in a conductance-based leaky integrate-and-fire neuron model with balanced excitatory and inhibitory synaptic input

A. N. Burkitt, H. Meffin, D. B. Grayden

The Bionic Ear Institute, 384–388 Albert Street, East Melbourne, Vic 3002, Australia

Abstract. Neurons receive a continual stream of excitatory and inhibitory synaptic inputs. A conductance-based neuron model is used to investigate how the balanced component of this input modulates the amplitude of neuronal responses. The output spiking rate is well described by a formula involving three parameters: the mean μ and variance σ of the membrane potential and the effective membrane time constant τ_Q. This expression shows that, for sufficiently small τ_Q, the level of balanced excitatory-inhibitory input has a nonlinear modulatory effect on the neuronal gain.

1 Introduction

Gain modulation is a change in the amplitude of the response that a neuron generates in response to an additional stream of input (the modulatory one) but that does not affect the receptive field characteristics (or selectivity) of the neuron. It provides a nonlinear mechanism by which information is combined between different pathways of neural processing, which may be of sensory, motor, or cognitive origin. Gain modulation has been shown experimentally to play a role in sensory-motor integration, such as eye and reaching movements, and in spatial perception as well as auditory masking, attentional processing, object recognition, and navigation (Salinas and Thier 2000). Experimental studies have established gain modulation as one of the important unifying computational principles in the brain, pervading multiple functions and brain areas (Salinas and Sejnowski 2001).

Although experimental studies have shown that gain modulation plays an important role in neural processing, our understanding of the underlying biophysical mechanisms by which neural systems implement gain modulation is lacking. The central question is, how do neurons achieve the nonlinear, multiplicative behavior characteristic of gain modulation when their input-output relationship is basically integrative? A number of possible different mechanisms have been proposed (Salinas and Thier 2000): nonlinear interactions in the dendritic processing of neurons (Mel 1993), nonlinear interactions arising from recurrent connections between neurons (Salinas and Abbott 1996; Hahnloser et al. 1999), correlations in the synaptic input (Salinas and Sejnowski 2000), and nonlinear responses modulated by the balanced component of the synaptic input (Chance et al. 2002).

This paper examines the mechanisms by which balanced synaptic input modulates neuronal gain. Balanced excitatory and inhibitory synaptic inputs have received particular attention recently (Shadlen and Newsome 1994; Tsodyks and Sejnowski 1995; van Vreeswijk and Sompolinsky 1996; Troyer and Miller 1997; Hohn and Burkitt 2001) since the variability in the spike times of such models agrees well with that observed in cortical neurons (Softky and Koch 1993; Shadlen and Newsome 1994, 1998). The possible role of balanced input in neuronal gain modulation was highlighted by a recent in vitro study in which a variable current (with zero mean) was injected into a rat cortical pyramidal neuron and the gain associated with the injection of an additional constant current was measured (Chance et al. 2002). The results indicated that the variability of the injected current affected the neuronal gain multiplicatively. In this paper, an analytic expression is derived for the output spiking rate of a conductance-based integrate-and-fire neuron. This enables us to identify the conditions under which the output spiking rate is modulated by the balanced input.

2 The conductance-based leaky integrate-and-fire neuron model

A one-compartment conductance-based leaky integrate-and-fire neuron is used in which the membrane potential $V(t)$ is the integrated activity of its excitatory and

Correspondence to: A. N. Burkitt
(e-mail: a.burkitt@medoto.unimelb.edu.au)

inhibitory synaptic inputs, and it decays in time with a characteristic time constant (Tuckwell 1979, 1989; Troyer and Miller 1997; Salinas and Sejnowski 2000; Tiesinga et al. 2000; Destexhe et al. 2001):

$$dV = -\frac{(V - v_0)}{\tau}dt + g_I(V_I - V)dP_I$$
$$+ g_E(V_E - V)(dP_E + dP_D) \tag{1}$$

The first term models the passive leak of the membrane, with resting potential v_0 and membrane time constant τ. The second and third terms represent the synaptic contribution due to cortical background activity from excitatory (dP_E) and inhibitory (dP_I) neurons, respectively. In the balanced neuron considered here, the net contribution of the background activity is approximately zero because the average values of these excitatory and inhibitory terms are chosen to approximately cancel each other out. In addition to the background activity, there is a synaptic driving current modeled as an excitatory fourth term (dP_D). The inputs dP_E, dP_I, dP_D are independent temporally homogeneous Poisson processes with constant intensities $\gamma_E = N_E\lambda_E$, $\gamma_I = N_I\lambda_I$, and $\gamma_D = N_D\lambda_D$ respectively, i.e., each of the N_E excitatory input fibers (resp. N_I inhibitory, N_D driving input fibers) has a spiking rate λ_E (resp. λ_I, λ_D). V_E and V_I are the (constant) reversal potentials ($V_I \leq v_0 \leq V(t) \leq V_{th} < V_E$). The parameters g_E and g_I represent the integrated conductances over the time course of the synaptic event divided by the neural capacitance (and are thus dimensionless): they are non-negative and are taken here to be identical for all excitatory and inhibitory inputs, respectively. When the membrane potential reaches a threshold V_{th}, an output spike is generated and the membrane potential is reset to its resting value v_0.

In the absence of spike generation, the membrane potential approaches an equilibrium value, μ, about which it fluctuates with variance σ^2. The membrane potential approaches μ with a time constant that is different from the passive membrane time constant due to the effect of the synaptic conductances, which is called the *effective* membrane time constant τ_Q. The values of μ, σ, τ_Q are (Hanson and Tuckwell 1983, Burkitt 2001)

$$\mu = \frac{v_0/\tau + r_{11}}{1/\tau_Q}$$

$$\sigma^2 = \frac{\mu^2 r_{20} - 2\mu r_{21} + r_{22}}{2/\tau_Q - r_{20}} \tag{2}$$

$$\frac{1}{\tau_Q} = \frac{1}{\tau} + r_{10}$$

$$r_{mn} = (\gamma_E + \gamma_D)g_E^m V_E^n + \gamma_I g_I^m V_I^n$$

The analysis is carried out in the Gaussian approximation (Burkitt and Clark 2000), in which the probability density of the membrane potential $p(v, t|v', 0)$ is parameterized as

$$p(v, t|v', 0) = \frac{1}{\sqrt{2\pi\Gamma(t; v')}}\exp\left\{-\frac{(v - \Upsilon(t; v'))^2}{2\Gamma(t; v')}\right\} \tag{3}$$

where $\Upsilon(t; v)$ and $\Gamma(t; v)$ are the (time-dependent) mean and variance of the membrane potential. The Gaussian approximation is accurate in the limit of a large number (N) of small-amplitude synaptic inputs, which allows the probability density of the membrane potential to be evaluated using a self-consistent analysis (Burkitt 2001). The output spike distribution $f_\theta(t)$ obeys the renewal equation (Plesser and Tanaka 1997; Burkitt and Clark 1999)

$$p(V_{th}, t|v_0, 0) = \int_0^t dt' f_\theta(t')p(V_{th}, t|V_{th}, t') \tag{4}$$

where $p(v, t|v', t')$ is the conditional probability density of the membrane potential having the value v at time t, given that it had the value v' at an earlier time t' (this equation is exact when the synaptic current is modeled as a series of delta functions; otherwise it is approximate).

The output spiking rate is determined from the average interspike interval

$$\lambda_{out} = \left[\tau_a + \int_0^\infty t\, f_\theta(t)dt\right]^{-1} \tag{5}$$

where τ_a is the absolute refractory period (taken to be zero here). The above integral is evaluated using Laplace transforms, where the Laplace transform for $f_\theta(t)$ is obtained from Eq. 4 using the time-translation invariance $p(v, t|v', t') = p(v, t - t'|v', 0)$. The time-dependent mean and variance are given by (see Sect. 2.3 of Burkitt 2001)

$$\Upsilon(t; v_0) = \mu\left(1 - e^{-t/\tau_Q}\right)$$
$$\Gamma(t; v_0) = \sigma^2\left(1 - e^{-2t/\tau_Q}\right) \tag{6}$$

where r_{20} is neglected in comparison with r_{10} in the exponent of $\Gamma(t; v_0)$. Careful consideration of the finite and divergent parts of the resultant integrals gives the output spiking rate, as shown in the appendix:

$$\lambda_{out}^{-1} = \frac{\tau_Q}{\sigma}\sqrt{\frac{\pi}{2}}\int_{v_0}^{V_{th}} du\, \exp\left(\frac{(u - \mu)^2}{2\sigma^2}\right)\left[1 + erf\left(\frac{u - \mu}{\sigma\sqrt{2}}\right)\right] \tag{7}$$

This is the so-called Siegert formula (Siegert 1951; Ricciardi 1977; Tuckwell 1988; Amit and Tsodyks 1991), but with the membrane time constant τ replaced by the effective time constant τ_Q. Note that once the parameters V_{th} and v_0 have been chosen, this formula gives the mean spiking rate as a function of the three variables μ, σ, and τ_Q, which are experimentally accessible (Inoue et al. 1995; Destexhe and Paré 1999).

3 Results

Background spiking activity in the cortex is reported to occur in the range of 5–20 Hz (Abeles 1991). To investigate the effect of the level of background activity

on the modulation of neuronal gain, 1.5× and 2× conditions were defined, corresponding to an increase by factors of 1.5 and 2, respectively, in the background activity (termed the 1× condition). The 1× condition was defined by choosing parameters μ, σ, and τ_Q in Eq. 7 so that a spiking rate of 5 Hz results from balanced background activity without a driving input. The effect upon neuronal gain was investigated by introducing driving input with spiking rate γ_D.

An essential part of the analysis was defining the "normal operating regime" of a neuron to ensure that the chosen parameter values correspond to biologically relevant neural behavior. The values of potentials were chosen to be $V_E = 0$ mV, $V_I = -80$ mV, $v_0 = -70$ mV, $V_{th} = -55$ mV, and the passive membrane time constant was $\tau = 20$ ms. These values accord with well-established measurements for cortical pyramidal neurons, and our results are not sensitive to variation of these potentials within the biologically plausible range. The experimentally accessible quantities μ, σ, and τ_Q (Destexhe and Paré 1999) to be investigated were defined by first establishing appropriate ranges in the 1× condition without driving input. These were: $(\mu - v_0)/\theta \in [0.0, 1.0]$, $\sigma/\theta \in [0.01, 1.0]$, and $\tau_Q/\tau \in [0.001, 1.0]$, where $\theta = V_{th} - v_0$. A set of triplets (μ, σ, τ_Q) were chosen that covered this region, with the constraint that their resultant output firing rate was $\lambda_{out} = 5$ Hz. For each triplet $\{(\mu, \sigma, \tau_Q)|\lambda_{out} = 5\,\text{Hz}\}$ the set of values of g_E, g_I, γ_E, and γ_I that could give rise to the triplet were inferred from Eq. 2. An upper bound on g_E was set by the requirement that at least 20 synaptic inputs were required for the neuron to reach threshold from the reset potential v_0 (and g_E, $g_I > 0$). Cortical neurons receive at least 1000 synaptic inputs, and the spontaneous (input) spiking rates λ_E, λ_I have a lower bound of 1 Hz (Abeles 1991). This procedure provided a finite space of parameters g_E, g_I, γ_E, and γ_I capable of accounting for the range of plausible values μ, σ, and τ_Q in the 1× condition with no driving input. The 1.5× and 2× conditions were obtained by increasing the values of γ_E and γ_I appropriately.

To investigate how the level of balanced background activity affects neuronal gain, the output spiking rate was plotted as a function of driving current in the 1×, 1.5×, and 2× conditions for the full range of biologically plausible parameters identified. The results revealed two qualitatively different behaviors (Fig. 1). The first type (Fig. 1a) was characterized by a linear response to driving input for all three conditions over most of the range of biologically relevant output spiking rates (taken here to be 5–120 Hz). The figure shows some deviation from linearity in the 1× condition for low output spiking rates (5–30 Hz). The effect of increased balanced background activity was simply to increase the spiking rate by a fixed amount, independent of the driving spiking rate γ_D. There was little effect on the gain, which remained approximately constant for all three conditions and most values of the driving spiking rate (Fig. 1b). This type of behavior was expected when the equilibrium potential was above threshold. Remarkably, however, this behavior could occur even if the equilibrium potential was below threshold (see inset to Fig. 1a,
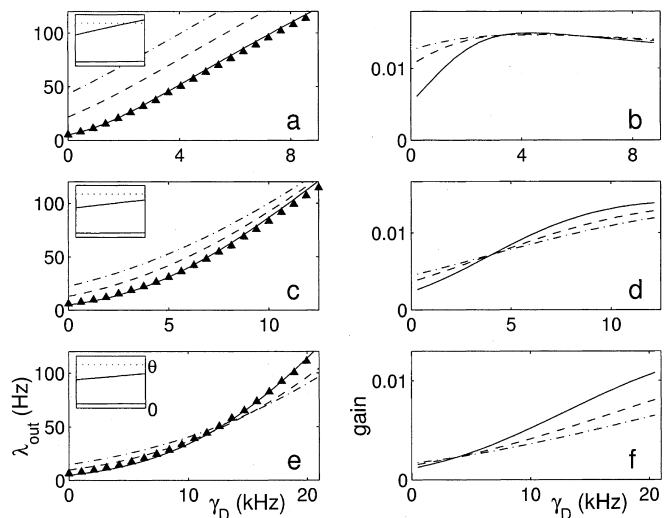

Fig. 1. Plots of the neuronal gain: plots on left show output spiking rate, λ_{out} (5) vs. spiking rate of driving inputs γ_D for three typical sets of neural parameters, and plots on right show the corresponding gain vs. γ_D. Results are shown for the 1× (*solid line*), 1.5× (*dashed line*), and 2× (*dot-dashed line*) conditions. The results of numerical simulations in the 1× condition with 10,000 output spikes are plotted as *triangles*. The insets in the left column show the corresponding values of μ (*upper solid line*) and σ (*lower solid line*), as well as the spiking threshold (*dotted line*), vs. γ_D for the 1× condition (same range as corresponding larger plot in each case). Parameter values for the 1× condition are: **a,b** $g_E = 0.0027$, $g_I = 0.0092$, $\gamma_E = 21.6$ kHz, $\gamma_I = 15.4$ kHz (i.e., $\tau_Q = 4$ ms), **c,d** $g_E = 0.0026$, $g_I = 0.0080$, $\gamma_E = 62.9$ kHz, $\gamma_I = 56.4$ kHz (i.e., $\tau_Q = 1.5$ ms), and **e,f** $g_E = 0.0026$, $g_I = 0.0079$, $\gamma_E = 143$ kHz, $\gamma_I = 137$ kHz (i.e., $\tau_Q = 0.67$ ms). Remaining neural parameter values are given in the text

showing μ and σ relative to θ). The second type of behavior (Fig. 1e) also exhibited an additive effect on the output spiking rate but was further characterized by a nonlinear response to driving input and a modulation in gain due to varying levels of background activity. Figure 1e shows that in the absence of driving input, increases in the level of balanced background activity caused increased spiking rates, as in the first type of behavior. However, there was a modulation of gain such that it decreased as the background activity increased (Fig. 1f). There was also intermediate behavior between these two types (Fig. 1c) in which the response to driving input was initially nonlinear but became linear as γ_D increased. In this case, there was a difference in the gain between the 1× and 2× conditions provided that the driving spiking rate was not so high as to put the 2× condition into the linear regime. To a first approximation, the types of behavior may be well characterized according to the value of τ_Q. Given a biologically relevant range of output spiking rates from 5 Hz (spontaneous activity) to 120 Hz (maximally driven output), linear behavior occurred across this entire range for $\tau_Q \sim 20$ ms (the upper bound of τ_Q, since $\tau_Q < \tau = 20$ ms for the parameters chosen here), while nonlinear behavior with gain modulation occurred across the range if $\tau_Q \leq 1$ ms. For 1ms $\leq \tau_Q \leq 20$ ms, intermediate behavior occurred: the crossover point from linear to nonlinear behavior (e.g., in Fig. 1a the linear regime was

for $\lambda_{\text{out}} > 30$ Hz) occurred at a value of λ_{out} that was inversely related to τ_Q. The gain modulation for values of τ_Q less than ~ 1 ms, as illustrated in Fig. 1e,f, became more multiplicative-like when the spontaneous output spiking rate (with $\gamma_D = 0$) was much lower than 5 Hz, as reported in Chance et al. (2002), but such low levels of spontaneous activity are outside the normal operating regime of cortical neurons. The change between linear and nonlinear behavior also depended somewhat on the value of σ, which is discussed below.

Figure 1 also shows the results of numerical simulations of the output spiking rate (shown by triangles on the plots for the $1\times$ condition). The numerical simulations were implemented by generating arrival times of the excitatory and inhibitory synaptic inputs according to Poisson distributions. The delta-function synaptic currents allow an exact update rule in which the membrane potential need only be evaluated at the synaptic input times. The results of numerical simulations show excellent agreement with those of the analytical expression for the parameters chosen here. The analytic expression for the output spiking rate (Eq. 7) was derived by considering only terms up to second order in g_E and g_I. Consequently this expression is most accurate for small values of these parameters (i.e., a large number of small-amplitude synaptic inputs, where the amplitude is measured in relation to the difference between the reset and threshold potentials), which is the case for most of the biologically relevant parameter range.

All the results given above are essentially the same if the synaptic driving input, which is stochastic, is replaced by a steady injected current with the same value as the mean synaptic driving current: $I_D =$
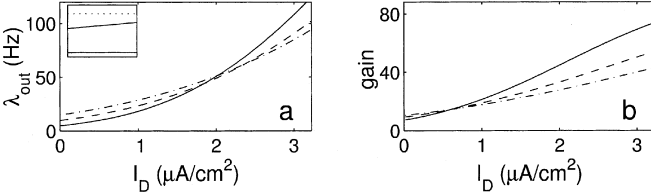
$C_m \gamma_D g_E (V_E - \mu)$, where C_m is the capacitance per-unit area of the membrane (taken to be $1\mu\text{F/cm}^2$). This is illustrated in Fig. 2, which shows data corresponding to Fig. 1e and f in the case of injected current. The results are nearly identical to those with synaptic driving input, indicating that the stochastic nature of the driving input γ_D (but not the background input, γ_E, γ_I) was unimportant in the behavior described here. This is unsurprising since $\gamma_D \ll \gamma_E$, γ_I. Consequently, the driving input contributes comparatively little to the fluctuations in the membrane potential.

To further understand the conditions that characterize the linear and nonlinear behavior, Eq. 5 was reparameterized as

$$\lambda_{\text{out}} = \frac{1}{\tau_Q} F\left(\frac{\mu - V_{\text{th}}}{\sqrt{2}\sigma}; \frac{\sigma}{\theta}\right)$$

$$= \frac{1}{\tau_Q}\left[\int_{-\frac{(\mu - V_{\text{th}})}{\sqrt{2}\sigma} - \frac{\theta}{\sqrt{2}\sigma}}^{-\frac{(\mu - V_{\text{th}})}{\sqrt{2}\sigma}} du\sqrt{\pi}e^{u^2}(1 + \text{erf}u)\right]^{-1} \quad (8)$$

Figure 3 shows that the function F is approximately linear in the first argument provided that the argument is greater than $-c$ and nonlinear otherwise. The value of c is in the range $[0.5, 1.5]$ depending on the strictness of the criteria for linearity and the ratio σ/θ (the smaller this ratio, the larger the value of c). This result has two important implications. First, a linear input-output curve does not require that the mean membrane potential μ exceed threshold, but rather that $\mu + \sqrt{2}c\sigma > V_{\text{th}}$. This provides a first criterion to determine whether gain modulation is present since it specifies when the nonlinear behavior occurs. Second, the transition from linear to nonlinear behavior occurs when the output spiking rate becomes larger than $\lambda_{\text{out}}^* = F(-c, \sigma/\theta)/\tau_Q$, where $0.07 \leq F(-c, \sigma/\theta) \leq 0.3$, as illustrated in Fig. 3b. This provides a second criterion for the presence of gain modulation behavior that relates directly to the output spiking rate. For example, a value of c in the middle of this range ($F(-c, \sigma/\theta) \approx 0.12$) produces linear behavior over the range $\lambda_{\text{out}} = 5$–120 Hz for $\tau_Q \geq 20$ ms and nonlinear behavior for $\tau_Q \leq 1$ ms, which is consistent with the above observation. These limiting values of τ_Q, for which purely linear or purely nonlinear behavior occurs, increase as σ/θ increases because this gives a smaller value of c that in turn produces a larger value of $F(-c, \sigma/\theta)$ (see Fig. 3a).

Fig. 2. Plots of neuronal gain for steady injected current $I_D = C_m \gamma_D g_E(V_E - \mu_{1X})$ with parameters as for Fig. 1e and f. $C_m = 1\mu\text{F/cm}^2$ is the capacitance of the neural membrane, and $\mu_{1X} = -60.175$ mV is the mean membrane potential in the $1\times$ condition without any driving input. **a** The output spiking rate, λ_{out} (Eq. 5), vs. I_D for three typical sets of neural parameters. **b** The corresponding gain vs. I_D. Results are shown for the $1\times$ (*solid line*), $1.5\times$ (*dashed line*), and $2\times$ (*dot-dashed line*) conditions
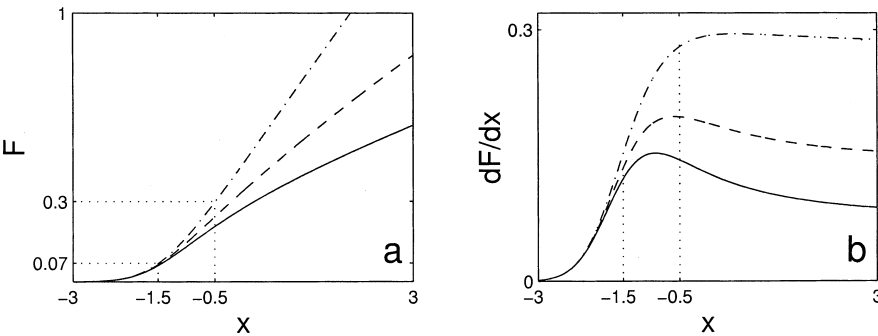

Fig. 3. a The function F, Eq. 8, and **b** its derivative with respect to its first argument $x = (\mu - V_{\text{th}})/\sqrt{2}\sigma$ for several values of its second argument $\sigma/\theta = 0.05$ (*solid*), 0.1 (*dashed*), and 0.2 (*dot-dashed*). The *vertical dotted lines* in **b** illustrate the region $-1.5 \leq \times \leq -0.5$ in which a transition from nonlinearity to linearity occurs, depending on the values of σ/θ and the strictness of the criteria for linearity. The *dotted lines* in **a** give the corresponding region and values of the function F

4 Discussion and conclusions

The effect upon gain modulation of increasing the balanced background activity can be understood in terms of two competing processes embodied in Eq. 8, both influenced by the effective membrane time constant, τ_Q. First, the contribution of a driving input to the mean membrane potential, μ_D, is approximately linear in γ_D, namely, $\mu_D = \gamma_D g_E \tau_Q V_E$ from Eq. 2. As the level of background activity increases, the effective time constant, τ_Q, decreases, resulting in a lower value of μ for a given driving spiking rate, γ_D. This decrease in τ_Q is due to the neuron becoming more leaky as more synaptic channels open (Tiesinga et al. 2000). The value of σ remains approximately constant for all conditions and driving spiking rates, also as a result of the increased leakiness. Although lower values of μ are expected to decrease the output spiking rate, this is offset by a second effect: the neuron operates on a faster time scale as τ_Q decreases, and so the time course and fluctuations in the membrane potential are more rapid. From Eq. 8, when the neuron is in the linear regime, these two competing effects approximately cancel and there is no gain modulation. When the neuron is in the nonlinear regime, the effect of the extra leakiness dominates over the effect of the faster time scale, resulting in diminished gain as the level of background activity increases.

The relative strength of these two opposing effects in different parameter regions explains many of the the differing results on gain modulation reported by a number of authors (Nelson 1994; Carandini and Heeger 1994; Holt and Koch 1997; Tiesinga et al. 2000; Capaday 2002; Longtin et al. 2002; Chance et al. 2002). The lack of gain modulation in the linear regime was first noted by Holt and Koch (1997), and a recent study of motoneurons (Capaday 2002) showed no gain modulation since they operate in the linear regime. The explanation of the linear behavior in these papers is based upon approximating the spiking rate by the inverse of the mean time taken for the membrane potential to reach threshold when only the mean input is considered (i.e., the stochastic nature of the changes to the membrane potential is ignored). When the membrane fluctuations are incorporated, this approximation remains valid only if the equilibrium membrane potential, μ (Eq. 2), is close to or above the spiking threshold. As the discussion following Eq. 8 indicates, such models correspond to the linear regime of the function F where no gain modulation is observed. The analysis presented here provides a quantitative prediction of the parameter regime in which the balanced component of the synaptic input gives rise to nonlinear gain modulation of the spiking rate and indicates that such conditions are within the biologically plausible region of cortical neurons.

The distinction between the signal input and the background (modulatory) input is based not on any anatomical difference but rather on the particular function that the synaptic input plays. For neurons in the nonlinear regime, the results here indicate that higher levels of balanced excitation and inhibition will produce a lower response gain in the output spiking rate of the neuron. Important questions that remain include whether a balance of excitatory and inhibitory synaptic input exists in vivo, whether the level of balanced input can be modulated in a behaviorally functional way, and whether such balanced synaptic input arises from feed-forward, recurrent, or feedback networks. Indirect evidence for balanced synaptic input in vivo is provided by the irregular spiking of cortical neurons (Shadlen and Newsome 1994). The large observed values of the coefficient of variation of the interspike interval distribution is inconsistent with the integration of a large number of small-amplitude postsynaptic potentials (Softky and Koch 1993) unless the neurons receive roughly balanced amounts of excitatory and inhibitory synaptic input (Shadlen and Newsome 1998). The question of whether such balanced input can be modulated in a functionally significant way in cortical neurons is much less clear. Indirect experimental support for a feedback source of balanced synaptic input is provided by studies on the primary visual cortex of monkeys in response to drifting grating stimuli in which the contrast, orientation, and spatiotemporal frequencies were varied (Carandini and Heeger 1994). The analysis presented here provides a neural mechanism for the nonlinear response observed in these studies without the need for the proposed "normalization" synaptic conductances that were postulated in their normalization model of gain modulation (in which a nonlinear neural response is generated by the interaction of a neuron with the pooled activity of a large number of nearby neurons) (Carandini and Heeger 1994). More recent models of gain modulation have also used recurrent and feedback interactions (Salinas and Abbott 1996; Hahnloser et al. 1999).

In conclusion, the results presented here give a quantitative picture of the extent to which neuronal gain can be modulated by the balanced component of the synaptic input for neurons with biologically realistic parameters. This analysis highlights the role played by the effective time constant, τ_Q, which results from the increased leakiness of the membrane as the balanced synaptic input increases (Tiesinga et al. 2000). Consequently, increases in the variance of the synaptic input do not necessarily cause corresponding increases in the variance of the membrane potential. The effect of gain modulation becomes most pronounced for τ_Q at less than approximately 1 ms, where increased levels of background activity produce a lower neural gain over most of the output spiking-rate range. Therefore, it is in this region that the gain modulation produced by the balanced synaptic input will potentially have the greatest functional significance, although the boundary of the region will depend on the ratio σ/θ.

Appendix: Derivation of the Siegert formula

In this appendix, the Siegert formula is derived for the leaky integrate-and-fire neuron with reversal potentials in the Gaussian approximation. The renewal equation (Eq. 4) may be solved for the first-passage time density, $f_\theta(t)$, using Laplace transforms:

$$f_L(s) = \frac{p_L(s)}{q_L(s)} \tag{9}$$

where the subscript L denotes the Laplace transform and $p_L(s)$ and $q_L(s)$ are the Laplace transforms of the probability density of the membrane potential, $p(v, t|v', 0)$:

$$p_L(s) = \int_0^\infty dt \, e^{-st} p(V_{th}, t|v_0, 0) \tag{10}$$

$$q_L(s) = \int_0^\infty dt \, e^{-st} p(V_{th}, t|V_{th}, 0) \tag{11}$$

Using Eq. 5 the mean firing rate can be calculated from the mean ISI, t_f, given by

$$t_f = \int_0^\infty t \, f_\theta(t) dt = \frac{p_L(0)q_L'(0) - p_L'(0)q_L(0)}{q_L(0)p_L(0)} \tag{12}$$

The integrals in Eqs. 10 and 11 and their derivatives can be rewritten using the Gaussian approximation for $p(v, t|v', 0)$ (Eqs. 3 and 7) with the change of variable $x = \exp(-t/\tau_Q)$

$$\frac{d^n}{ds^n} p_L(s) = \int_0^1 dx (\tau_Q \ln x)^n \frac{\tau_Q x^{\tau_Q s - 1}}{\sqrt{2\pi\sigma^2(1 - x^2)}}$$
$$\times \exp\left\{-\frac{(y_{th} - y_r x)^2}{1 - x^2}\right\} \tag{13}$$

$$\frac{d^n}{ds^n} q_L(s) = \int_0^1 dx (\tau_Q \ln x)^n \frac{\tau_Q x^{\tau_Q s - 1}}{\sqrt{2\pi\sigma^2(1 - x^2)}}$$
$$\times \exp\left\{-\frac{y_{th}^2(1 - x)^2}{1 - x^2}\right\} \tag{14}$$

where $y_{th} = (V_{th} - \mu)\sqrt{2}\sigma$, $y_r = (v_0 - \mu)\sqrt{2}\sigma$. In the limit as $s \to 0$ these integrals are divergent (the integrand is singular at $x = 0$) and can be written in terms of finite and singular parts

$$\frac{d^n}{ds^n} p_L(s) = \frac{\tau_Q}{\sqrt{2\pi\sigma^2}}\left[p_F(s; n) + \frac{(-1)^n n! \exp(-y_{th}^2)}{\tau_Q s^{n+1}}\right] \tag{15}$$

$$\frac{d^n}{ds^n} q_L(s) = \frac{\tau_Q}{\sqrt{2\pi\sigma^2}}\left[q_F(s; n) + \frac{(-1)^n n! \exp(-y_{th}^2)}{\tau_Q s^{n+1}}\right] \tag{16}$$

where $p_F(s; n)$ and $q_F(s; n)$ are the finite parts of $p_L(s)$ and $q_L(s)$, respectively,

$$p_F(s; n) = \int_0^1 dx (\tau_Q \ln x)^n \frac{x^{\tau_Q s - 1}}{\sqrt{(1 - x^2)}}$$
$$\times \left[\exp\left\{-\frac{(y_{th} - y_r x)^2}{1 - x^2}\right\} - \exp(-y_{th}^2)\sqrt{(1 - x^2)}\right] \tag{17}$$

$$q_F(s; n) = \int_0^1 dx (\tau_Q \ln x)^n \frac{x^{\tau_Q s - 1}}{\sqrt{(1 - x^2)}}$$
$$\times \left[\exp\left\{-\frac{y_{th}^2(1 - x)^2}{1 - x^2}\right\} - \exp(-y_{th}^2)\sqrt{(1 - x^2)}\right] \tag{18}$$

In Eq. 12 for the mean ISI, the singular parts cancel so that in the limit as $s \to 0$

$$t_f = \exp(y_{th}^2)\left(\int_0^1 dx \frac{\tau_Q x^{-1}}{\sqrt{(1 - x^2)}} \exp\left\{-\frac{y_{th}^2(1 - x)^2}{1 - x^2}\right\}\right.$$
$$\left. - \int_0^1 dx \frac{\tau_Q x^{-1}}{\sqrt{(1 - x^2)}} \exp\left\{-\frac{(y_{th} - y_r x)^2}{1 - x^2}\right\}\right) \tag{19}$$

Consider these two integrals separately and notice that the following related identities hold:

$$\frac{d}{du}\left[\exp(u^2) \int_0^1 dx \frac{x^{-1}}{\sqrt{(1 - x^2)}}\left(\exp\left\{-\frac{u^2(1 - x)^2}{1 - x^2}\right\}\right)\right]$$
$$= 4\exp(u^2) \int_0^u dz \exp(-z^2) \tag{20}$$

$$\frac{d}{du}\left[\exp(u^2) \int_0^1 dx \frac{x^{-1}}{\sqrt{(1 - x^2)}}\left(\exp\left\{-\frac{(u - y_r x)^2}{1 - x^2}\right\}\right)\right]$$
$$= -2\exp(u^2) \int_u^\infty dz \exp(-z^2) \tag{21}$$

Consequently,

$$t_f = \tau_Q \int_{y_r}^{y_{th}} du \exp(u^2)$$
$$\times \left(4 \int_0^u dz \exp(-z^2) + 2 \int_u^\infty dz \exp(-z^2)\right)$$

$$= \tau_Q \int_{y_r}^{y_{th}} du \exp(u^2)$$

$$\times \left(2 \left[\int_0^\infty dz \exp(-z^2) + \int_0^u dz \exp(-z^2) \right] \right)$$

$$= \sqrt{\pi} \tau_Q \int_{\frac{v_0 - \mu}{\sqrt{2}\sigma}}^{\frac{V_{th} - \mu}{\sqrt{2}\sigma}} du \exp(u^2)[1 + \mathrm{erf}(u)] \tag{22}$$

$$= \frac{\tau_Q}{\sigma} \sqrt{\frac{\pi}{2}} \int_{v_0}^{V_{th}} du \exp\left(\frac{(u - \mu)^2}{2\sigma^2} \right) \left[1 + \mathrm{erf}\left(\frac{u - \mu}{\sqrt{2}\sigma} \right) \right]$$

References

Abeles M (1991) Corticonics: neural circuits of the cerebral cortex. Cambridge University Press, New York

Amit DJ, Tsodyks MV (1991) Quantitative study of attractor neural network retrieving at low spike rates. I. Substrate – spikes, rates and neuronal gain. Netw Comput Neural Sys 2: 259–273

Burkitt AN (2001) Balanced neurons: analysis of leaky integrate-and-fire neurons with reversal potentials. Biol Cybern 85: 247–255

Burkitt AN, Clark GM (1999) Analysis of integrate-and-fire neurons: synchronization of synaptic input and spike output in neural systems. Neural Comput 11: 871–901

Burkitt AN, Clark GM (2000) Calculation of interspike intervals for integrate-and-fire neurons with Poisson distribution of synaptic inputs. Neural Comput 12: 1789–1820

Capaday C (2002) A re-examination of the possibility of controlling the firing rate gain of neurons by balancing excitatory and inhibitory conductances. Exp Brain Res 143: 67–77

Carandini M, Heeger DJ (1994) Summation and division by neurons in primate visual cortex. Science 264: 1333–1336

Chance FS, Abbott LF, Reyes AD (2002) Gain modulation from background synaptic input. Neuron 35: 773–782

Destexhe A, Paré D (1999) Impact of network activity on the integrative properties of neocortical neurons in vivo. J Neurophysiol 81: 1531–1547

Destexhe A, Rudolph M, Fellous JM, Sejnowski TJ (2001) Fluctuating synaptic conductances recreate in-vivo-like activity in neocortical neurons. Neuroscience 107: 13–24

Hahnloser R, Douglas RJ, Mahowald M, Hepp K (1999) Feedback interactions between neuronal pointers and maps for attentional processing. Nat Neurosci 2: 746–752

Hanson FB, Tuckwell HC (1983) Diffusion approximations for neuronal activity including synaptic reversal potentials. J Theor Neurobiol 2: 127–153

Hohn N, Burkitt AN (2001) Shot noise in the leaky integrate-and-fire neuron. Phys Rev E 63: 031902

Holt GR, Koch C (1997) Shunting inhibition does not have a divisive effect on firing rates. Neural Comput 9: 1001–1013

Inoue J, Sate S, Ricciardi LM (1995) On the parameter extimation for diffusion models of single neuron's activities. Biol Cybern 73: 209–221

Longtin A, Doiron B, Bulsara AR (2002) Noise induced divisive gain control in neuron models. BioSystems 67: 147–156

Mel BW (1993) Synaptic integration in an excitable dendritic tree. J Neurophysiol 70: 1086–1101

Nelson ME (1994) A mechanism for neuronal gain control by descending pathways. Neural Comput 6: 242–254

Plesser HE, Tanaka S (1997) Stochastic resonance in a model neuron with reset. Phys Lett A 225: 228–234

Ricciardi LM (1977) diffusion processes and related topics in biology. Springer, Berlin Heidelberg New York

Salinas E, Abbott LF (1996) A model of multiplicative neural response in parietal cortex. Proc Natl Acad Sci USA 93: 6461–6474

Salinas E, Sejnowski TJ (2000) Impact of correlated synaptic input on output firing rate and variability in simple neuronal models. J Neurosci 20: 6193–6209

Salinas E, Sejnowski TJ (2001) Gain modulation in the central nervous system: where behavior, neurophysiology and computation meet. Neuroscientist 7: 430–440

Salinas E, Thier P (2000) Gain modulation: a major computational principle of the central nervous system. Neuron 27: 15–21

Shadlen MN, Newsome WT (1994) Noise, neural codes and cortical organization. Curr Opin Neurobiol 4: 569–579

Shadlen MN, Newsome WT (1998) The variable discharge of cortical neurons: implications for connectivity, computation, and information coding. J Neurosci 18: 3870–3896

Siegert AJF (1951) On the first passage time probability problem. Phys Rev 81: 617–623

Softky WR, Koch C (1993) The highly irregular firing of cortical cells is inconsistent with temporal integration of random EPSPs. J Neurosci 13: 334–350

Tiesinga PHE, José JV, Sejnowski TJ (2000) Comparison of current-driven and conductance-driven neocortical model neurons with Hodgkin-Huxley voltage-gated channels. Phys Rev E 62: 8413–8419

Troyer TW, Miller KD (1997) Physiological gain leads to high ISI variability in a simple model of a cortical regular spiking cell. Neural Comput 9: 971–983

Tsodyks MV, Sejnowski TJ (1995) Rapid state switching in balanced cortical network models. Netw Comput Neural Sys 6: 111–124

Tuckwell HC (1979) Synaptic transmission in a model for stochastic neural activity. J Theor Biol 77: 65–81

Tuckwell HC (1988) introduction to theoretical neurobiology, vol 2, Nonlinear and stochastic theories. Cambridge University Press, Cambridge

Tuckwell HC (1989) Stochastic processes in the neurosciences. Society for Industrial and Applied Mathematics, Philadelphia

Van Vreeswijk C, Sompolinsky H (1996) Chaos in neuronal networks with balanced excitatory and inhibitory activity. Science 274: 1724–1726